Temperature-induced recovery of a bioactive enzyme using polyglycerol dendrimers: correlation between bound water and protein interaction

Ooya, Tooru

Ogawa, Takaya

Takeuchi, Toshifumi

(Citation)
Journal of Biomaterials Science, Polymer Edition,29(6):701-715

(Issue Date)
2018

(Resource Type)
journal article

(Version)
Accepted Manuscript

(URL)
https://hdl.handle.net/20.500.14094/90004808

Temperature-Induced Recovery of a Bioactive Enzyme Using Polyglycrol Dendrimers: Correlation between Bound Water and Protein Interaction

Tooru Ooya*, Takaya Ogawa, and Toshifumi Takeuchi*

Graduate School of Engineering, Kobe University, 1-1 Rokkodai-cho, Nada-ku, Kobe 657-8501, Japan

*Authors to whom correspondence should be addressed;

E-mail: ooya@tiger.kobe-u.ac.jp, takeuchi@gold.kobe-u.ac.jp

Tel.: +81-78-803-6255; Fax: +81-78-803-6255.

.

Temperature-Induced Recovery of a Bioactive Enzyme Using Polyglycrol Dendrimers: Correlation between Bound Water and Protein Interaction

Enzyme application has gained importance over the past decade in bioprocess, biomedical, and pharmaceutical fields. We found that polyglycerol dendrimers (PGDs), which are biocompatible molecules, can recover alcohol dehydrogenase (ADH) from aqueous solution under elevated temperature. A low concentration of PGD (5 wt.%) is sufficient for the recovery of high enzymatic activity, although a high concentration (25–75 wt.%) of glycerol is generally required to stabilize ADH. The enzymatic activity of ADH in suspension with PGDs is over 60% but it is only 10% in that with glycerol. The results of osmolarity and spin-lattice relaxation time (T_1) of water measurements in the presence of PGDs suggest that increased amounts of bound water to PGD molecules trigger aggregation along with the direct interaction with ADH. PGDs therefore represent good potential additives for direct recovery of enzymes from aqueous solutions.

Keywords: Alcohol Dehydrogenase; Polyglycerol Dendrimers; Bound water; Protein stability; Spin-lattice relaxation times

Introduction

Enzymes located at material–water interfaces have gained importance over the past decade in numerous fields, including surface chemistry[1], drug delivery[2], biosensing[3], and biocatalysts[4, 5, 6]. Major applications of enzymes are in medicine, textile industry, pharmaceutical industry, and food industry. Enzyme applications involving interactions with biomaterials often cause loss of biological activity through protein unfolding and/or aggregation at the interface[7]. Although enzymes display aspects such as catalyst functions for highly specific reactions under mild conditions, such potential advantages are lost by denaturation during storage, limiting enzyme applications in industry. Hence, enzymes with maintained or recovered activities could play important

roles in industrial uses. Various protein recovery techniques aimed for medical use have been devised, yet maintaining high levels of enzyme activity following recovery remains challenging.

Alcohol dehydrogenase (ADH) is a widely studied enzyme for biotechnology applications. Supporting materials are required to recover ADH because free ADH cannot be reused due to its lack of long term stability under processing conditions and that it is difficult to recover from the reaction mixture. When ADH is dissolved in aqueous solution, its thermal and chemical denaturation occurs because the folded structure is lost. Many researchers have used additives and preservatives, including poloxamer[8], trehalose[9, 10], and glycerol[11, 12, 13, 14, 15], to prevent protein unfolding and obstruction of the active sites upon recovery and reuse.

Glycerol is one of the most widely used low molecular weight solution additives that is effective in suppressing denaturation. Hydroxyl groups on glycerol are believed to exchange water-bound amino acids with hydrophilic amino acids located on the protein surface or to enhance hydrophobic interactions among hydrophobic amino acids in proteins. A high concentration (25–75 wt.%) of glycerol is required to obtain a good stabilizing effect[11, 12]. Leggewie and co-workers studied the effect of polyol additives, including glycerol, sorbitol, mannitol, salts, and PEG on the stability of ADH[16]. Deactivation of ADH was prevented at very high concentrations of these additives. The mechanism underlying stabilization remains unclear, but several possibilities have been suggested. For example, polyol compounds might enhance hydrophobic interactions among non-polar amino acid residues[17]. In general, osmolytes such as glycerol stabilize proteins by shifting the denaturation equilibrium from the denatured state to the native state, with the concentration of hydroxyl groups being a key parameter for determining the stabilizing effects of polyols[18]. Vandate et al. proposed that protein

stabilization by glycerol[14] implies that glycerol interacts with protein N and O atoms through multiple hydrogen bonds, followed by a conformational change in the protein. Furthermore, glycerol preferably interacts with hydrophobic surface regions by orienting the protein in a manner that increases solvent hydration, thereby preventing protein aggregation at the water interface.

Polyglycerol dendrimers (PGDs, **Fig. 1**) are dendrimers comprising glycerol units, which along with hyperbranched polyglycerols (HPGs) have been extensively studied for biomedical applications[19, 20, 21, 22, 23, 24, 25, 26, 27]. Unlike HPGs, PGDs are branched molecules with defined molecular weights[28] and thus support host–guest interactions in a stoichiometric manner[29, 30, 31, 32]. We have focused on PGDs as biomaterials rather than HPGs because of their perfect dendrimer characteristics: the degree of branching (DB) of PGDs is 100%, whereas that of HPGs is 50–60%[19]. The 100% DB leads to perfect functionalization of the periphery[33], which also results in perfect nanocoating on PMMA surface due to the densely packed functionalized groups that induce crystallization[34]. Considering the high functionalization performance, PGDs are likely to interact well with enzymes. Similar to HPGs, PGDs are known as nontoxic and biocompatible molecules. In addition, the weak amphiphilic nature[29, 30] of PGDs allows them to act as hydrotropic agents for solubilizing poorly soluble drugs[35, 36]: the high local density and number of hydroxyl groups of PGDs alters the hydration state of water and drug molecules. The influence of the densely packed hydroxyl groups and the branched nature of PGDs on enzyme activity remains unknown, although PGDs are expected to stabilize enzymes as well as glycerol.

Here we propose a strategy of recovery of ADH using PGDs in an aqueous solution by elevating temperature to recover ADH as a precipitate. PGD generation 1 (G1), 2 (G2), and 3 (G3) were synthesized and their cytotoxicities were evaluated by

colony formation assay. Even at a low concentration of PGDs (5 wt.%), elevated temperature induced aggregation containing ADH with high enzymatic activity. The underlying mechanism was discussed in the view points of ADH conformational change upon supplying heat energy and water condition, which was analyzed by circular dichroism, differential scanning calorimetry (DSC), osmolarity and spin-lattice relaxation times (T_1) of water measurements in the presence of PGDs. Our results provide an estimate of the water activity and the number of hydrated water molecules per PGD molecule. Temperature-induced ADH recovery using PGDs has good potential for bioprocess and biomedical engineering.

(insert Fig. 1)

Experimental

Materials

Allyl chloride, *N*-methylmorpholine *N*-oxide (NMO), 50 wt.% sodium hydroxide solution, and alcohol dehydrogenase from *Saccharomyces cerevisiae* (EC: 1.1.1.1) (ADH) were purchased from Sigma-Aldrich (Tokyo, Japan). 1,1,1-Tris (hydroxymethyl) propane (TMP) was purchased from Wako Pure Chemical Industries, Ltd. (Osaka, Japan). Tetrabutylammonium bromide and OsO_4 (4% in water) were purchased from Tokyo Chemical Industry Co. Ltd. (Tokyo, Japan). β-nicotineamide adenine dinucleotide from yeast (NAD^+), zinc chloride ($ZnCl_2$), t-butanol (t-BuOH), sodium sulfate (Na_2SO_4), and silica gel 60 (230–400 mesh) were purchased from Nacalai Tesque, Inc. (Kyoto, Japan). Glycerol was purchased from Kanto Chemical Co. Inc. (Tokyo, Japan). Acetone, petroleum ether, ethyl acetate, toluene, and methanol were of a reagent grade. Aluminium oxide 90 (active acidic) was purchased from Merck Ltd. (Tokyo, Japan).

Synthesis and Characterization of PGDs

PGD G1, G2, and G3 (**Fig. 1**) were synthesized and characterized according to previous reports[37, 38]. In brief, TMP used as a starting material was allylated by allyl chloride, which produced a PGD (G0.5). Then, subsequent catalytic dihydroxylation of the allylic double bond of PGD-G0.5 was performed in the presence of OsO_4 and NMO[37] to produce PGD-G1. PGD-G1 was purified by column chromatography using aluminium oxide 90 (active acidic) as a column carrier (eluent: methanol), followed by silica gel 60 (eluent: methanol: ethyl acetate = 5:5–10:0). In the same manner, PGD-G2 and G3 were obtained. The purification process allowed to remove osmium up to a sub-ppm order[19].

[PGD-G1]

^{1}H-NMR (300MHz, D_2O): 0.69(*t*,3H,CH_3), 1.21(*q*,2H,CH_3CH_2), 3.19(*s*,6H,$C(CH_2)_3$), 3.20-3.52(*m*,12H), 3.75(*m*,3H,CHOH); MALDI-TOF-MS (CHCA, 15000V, positive) m/z 379.2 [M+Na].

[PGD-G2]

^{1}H-NMR (300MHz, D_2O): 0.70(*t*,3H,CH_3), 1.22(*q*,2H,CH_3CH_2), 3.19(*s*,6H,$C(CH_2)_3$), 3.76-3.42 (*m*,45H); MALDI-TOF-MS (CHCA, 15000V, positive) m/z 824.4 [M+Na], 840.5 [M+K].

[PGD-G3]

^{1}H-NMR (300MHz, D_2O): 0.70(*t*,3H,CH_3), 1.23(*q*,2H,CH_3CH_2), 3.16(*s*,6H,$C(CH_2)_3$), 3.71-3.45(*m*,105H),; MALDI-TOF-MS (CHCA, 15000V, positive) m/z 1713.4 [M+Na], 1729.2 [M+K].

Cytotoxic assay

Cytotoxicity of PGDs was assayed by the colony formation method[38]. V79 cells were obtained from JCRB Cell Bank (Japan) and cultured in a CO_2 incubator (CO_2

concentration: 5%, 37°C) using an Eagle's MEM medium (MEM10 medium) containing 10 vol.% of fetal bovine serum (lot number: 24300133, Moregate). PGD-G2 and G3 were dissolved in water for injection (Otsuka Pharmaceutical Factory, Japan), and the maximum treatment concentration was adjusted to a physiological limit dose of 5 mg/mL. Treatment concentrations were prepared to be 0.0977, 0.195, 0.391, 0.781, 1.56, 3.13, 6.25, 12.5, 25.0, and 50.0 mg/ mL.

After isolating V79 cells with 0.25% trypsin, a suspension of 10^3 cells/ mL was prepared, and 0.1 mL (100 cells) of this concentration was added to a 6-well plate containing 2 mL of MEM 10 medium (Well diameter: 35 mm). The day after seeding, the medium in the well was removed and 1.8 mL of fresh MEM 10 medium was added. Either 200 μL water for injection (negative control) or the diluted test solution were added to the medium (solvent concentration 10 vol.%) and incubated in a CO_2 incubator (CO_2 concentration 5%, 37°C) for 6 days.

After completion, the medium was removed from the culture, and the cells were fixed with methanol and stained with 10 vol.% Giemsa solution. The number of colonies per well (one consisting of 50 or more cells was taken as one) was assessed with a multipurpose high-speed image analyzer (Model No.: PCA-11, System Science Co Ltd., Tokyo, Japan) and compared with the negative control group. The relative colony formation rate of the treated group was calculated, and the IC_{50} value was determined. As a positive control, zinc di-*n*-butyldithiocarbamate (ZDBC) was used, and the IC_{50} value was calculated in the same manner.

Turbidity measurements at 60℃

ADH was dissolved in 3 mL of 50 mM Tris–HCl buffer (pH 8.0) to be 0.7 or 10 μM in a quartz cell (optical length: 1 cm), then PGD-G1, G2, G3, or glycerol (150 mg) was added

to attain 5 wt.%. The solution was stirred using a stirrer bar at 60°C in a UV-Vis spectrophotometer (Jasco V-550, JASCO Corporation, Tokyo, Japan) equipped with a program controller that maintains the temperature or controls the speed of temperature change. Turbidity was determined by measuring the apparent absorbance at 600 nm for 250 s.

Enzymatic activity before and after heat treatment

Enzymatic activity was analyzed spectrophotometrically by recording incremental changes in absorbance at 340 nm due to the formation of NADH during the oxidation of ethanol[39]. One unit of enzymatic activity was defined as the amount of enzyme necessary to produce 1 µmol NADH/min. ADH activity before heat treatment was measured in the spectrophotometer using 2.7 mL of 50 mM Tris–HCl buffer (pH 8.0) containing 1 µM ADH, 100 µM NAD^+, 20 µM $ZnCl_2$, and 0.5 wt.% of each polymer (PGD-G1, G2, G3, or glycerol) under stirring in a quartz cell at room temperature. Absorbance measurements at 340 nm begun immediately at 25°C after adding 0.3 mL of 3 mM ethanol in Tris buffer, and absorbance was monitored for 3 min. Enzymatic activity after heat treatment at 60°C for 2 h was measured using the same conditions as described for turbidity measurements but using 10 µM ADH in 50 mM Tris–HCl buffer (pH 8.0) containing 150 mg of each polymer (PGD-G1, G2, G3, or glycerol) (3 mL) maintained at 60°C in a water bath for 2 h. An aliquot of the suspension (300 µL) was then removed and added to 2.4 mL of 50 mM Tris-HCl buffer (pH 8.0) containing 100 µM NAD^+ and 20 µM $ZnCl_2$ in a quartz cell at 60°C. Following the addition of 300 µL of 3 mM ethanol in Tris buffer, absorbance at 340 nm was measured immediately under stirring at 60°C in a water bath. Enzymatic activity (U/mg) was calculated from the obtained initial slope of the increase in absorbance at 340 nm to provide the initial reaction rate, where one unit of activity was defined as the amount of enzyme required to produce 1 µmol NADH/min.

The remaining sample following heat treatment at 60°C was centrifuged, and 300 μL of the supernatant was assayed for enzymatic activity in the same manner.

Residual ADH activity (%) after heat treatment in both the suspension and supernatant was calculated using the following equation:

$$\text{Residual ADH activity (\%)} = (\text{Activity after heat treatment}/\text{Activity before heat treatment}) \times 100$$

Determination of ADH concentration

The concentration of ADH in the supernatant after heat treatment was measured by the Bradford method using a Coomasie® Plus Protein Assay Reagent Kit (Thermo Fisher Scientific Inc., Yokohama, Japan). A calibration curve was prepared using ADH concentrations ranging from 0 to 2 mg/mL. Coomasie® Plus Reagent (1.5 mL) was added to the heat-treated supernatant, followed by incubation for 10 min at room temperature. The absorbance at 595 nm of each sample was measured. The recovery percentage of ADH was calculated by the following equation:

$$\text{Recovery of ADH (\%)} = [(\text{ADH in feed} - \text{ADH in the supernatant})/(\text{ADH in feed})] \times 100$$

Circular dichroism (CD) measurements

ADH (0.3 mg) was dissolved to 0.7 μM in 3 mL of 50 mM Tris–HCl buffer (pH 8.0) in a quartz cell (optical length: 1 cm), and each polymer (PGD-G1, G2, or G3) (30 mg) was added at 1 wt%. The samples were heated at 50°C in a water bath for 1 h, then CD spectra were measured every 10 min for 1 h using the following measurement conditions: wavelength: 250–195 nm, band width: 10 nm, response: 0.5 s, sensitivity: 200 mdeg, speed: 100 nm/min, and resolution: 0.2 nm. The change in molar ellipticity ([θ]) at 222 nm, which is an index of the α-helix content of a protein, was calculated using the following equation:

$$\Delta[\theta] = ([\theta] \text{ at elapsed time}) - ([\theta] \text{ at 0 min})$$

DSC measurements

DSC measurements of ADH dissolved in 10 mM PBS (pH 7.4) (final concentration: 0.7 μM) in the presence of PGD-G1, G2, or G3 (final concentration: 1 wt.%) were conducted using a Nano DSC (TA Instruments Japan, Inc., Tokyo, Japan). The prepared solutions were degassed for 15 min; then 0.3 mL of sample was pipetted into the platinum capillary cell. Temperature was increased from 15°C to 100°C at a scan rate of 1°C/min. The data were analyzed using Nano Analyze 2.2 software to determine the calorimetric enthalpy (ΔH_{cal}), the calorimetric entropy (ΔS_{cal}), and the midpoint temperature of the unfolding process (T_m).

Osmolarity measurements

The osmolarities of the polymer samples (0.8–6.3 wt.% (0.0046–0.68 M) of PGD-G1, G2, G3, or glycerol in 50 mM Tris–HCl buffer (pH 8.0)) with 0.1 mM ADH were determined using a Wescor osmometer (VAPRO 5520: Wescor Inc., Logan, UT, USA) calibrated with standard solutions of NaCl. A paper filter (sample discs SS-033 for use with the VAPRO 5520) was set in the sample chamber, then the filter was impregnated with 10 μL of sample, and osmolarity was measured for 80 s. Each measurement was repeated three times. The osmolarities of the polymer solutions alone (0.8–6.3 wt.% (0.0046–0.68 M) of PGD-G1, G2, G3, or glycerol in 50 mM Tris–HCl buffer (pH 8.0)) were measured in the same manner.

T_1 measurements

Each solution (PGD-G1, G2, G3 or glycerol; concentrations as shown in Table 1) was dissolved in D_2O/H_2O (95:5) (0.7 mL) and then degassed. T_1 measurements were

conducted using a 300-Hz FT-NMR apparatus (JNM-LA300 FT NMR SYSTEM, JEOL Ltd., Tokyo, Japan) to determine the number of polymer hydroxyl groups interacting per water molecule (N_{OH}) and the results are summarized in **Table. 1**. T_1 was measured at 25°C using the inversion recovery sequence $\pi - t - \pi/2$ at 15 times t values.

(insert **Table .1**)

Results and Discussion

PGDs were successfully synthesized as confirmed by the results of ^{1}H-NMR and MALDI-TOF-MS data (see Experimental). Cytotoxicities of the synthesized PGDs were assessed by colony formation assay that is known as a highly sensitive cytotoxicity test[38]. As shown in **Fig. 2**, PGDs did not inhibited colony formation of V79 cells, indicating negligible PGD cytotoxicities. In the concentration range of 0.001–5 mg/mL, IC_{50} values could not be calculated, although the IC_{50} value of ZDBC (positive control) was found to be 1.7 μg/mL. These results indicate that the synthesized PGDs are cytocompatible molecules.

(insert **Fig. 2**)

Enzymatic inactivation is usually accompanied by precipitation, and thus, the protective effects of PGDs on ADH stability during heat treatment were monitored based on turbidity changes. An ADH concentration at 0.7 μM provided turbidity measurement of 0% for over 60 min at 60°C, whereas at 10 μM, the turbidity increased gradually starting at 2.5 min (**Fig. 3**). The addition of PGD-G1, G2, G3, or glycerol to 10 μM ADH solution modulated turbidity change: PGDs enhanced the aggregation of ADH in the order PGD-G3 > G2 > G1, whereas glycerol suppressed ADH aggregation (**Fig. 3 (a)-(d)**). These results suggest that molecular interactions between PGD and ADH induced aggregation. The absolute rate of aggregation was proportional to the generation of PGDs. The molar

concentrations of PGD-G1, G2, and G3 were 0.14, 0.062, and 0.030 M, respectively, based on the concentration of hydroxyl groups in each PGD solution being 0.84, 0.74, and 0.72 M, respectively. Therefore, in each solution of 5 wt.% PGD, the concentration of hydroxyl groups was similar, and thus, the observed generation-dependent aggregation phenomena are likely correlated with polarity differences among PGDs in aqueous conditions[29, 30]. The recovery percentages of ADH in the precipitates were calculated by determining ADH concentration in the supernatant after the heat treatment (see: Experimental part). The ADH recovery % in each precipitation containing PGD-G1, G2, G3, and glycerol was calculated to be 96.7 ± 0.3, 87.6 ± 0.8, 93.6 ± 0.8, and 98.6 ± 0.3 %, respectively. Therefore, almost all initial ADH was recovered by elevating temperature in the precipitates.

(insert **Fig. 3**)

Residual ADH activity in the suspension following heat treatment at 60°C was determined by comparing with ADH activity before heat treatment (see: Experimental part). Surprisingly, heat treatment of ADH with or without glycerol in the suspension decreased activities to 10%–15%, whereas the presence of PGDs provided activity in the range of 43%–67% (**Fig. 4**). These results suggest that PGDs maintain the enzymatic activity of ADH even after aggregation. ADH activities measured in the supernatants following centrifugation of the suspension were below 10% (**Fig. 4**), further supporting that the observed ADH activity was due to ADH in the aggregated state. Consequently, over 60% of ADH activity was maintained following heating in the presence of only 5 wt.% of PGDs. Here, once again, the ADH activity was calculated by absorbance change attributed to the formation of NADH from NAD^+ during the oxidation of ethanol. The remaining ADH activity suggests that the NAD^+-binding domain (residues 176-318)

and/or the catalytic domain (residues 1–175, 319–374), which consists of β-sheet and α-helix[40], are not damaged after mixing with ADH. Therefore, from the view point of the secondary structure, the CD spectra were measured after the heat treatments.

(insert **Fig. 4**)

The CD spectra of ADH in the presence or absence of PGD-G1, G2, or G3 at 60°C were measured to gain insights into the conformational change of ADH in the presence of PGDs. The concentration of ADH was fixed at 0.7 μM because no precipitation occurred at this concentration at 60°C, as mentioned above. The CD spectra were monitored for 60 min (see Supporting information, Fig. SI-1), and the change in molar ellipticity at 222 nm ($\Delta[\theta]$) was plotted against time (**Fig. 5**). The $\Delta[\theta]$ values increased with the generation of PGDs, indicating that mixing with PGDs decreased the α-helix content of ADH. PGD-G3, which is the least polar in this series[30], induced an extreme conformational change, whereas the $\Delta[\theta]$ value of ADH in the absence of additive remained unchanged. These results suggest that the α-helix was unfolded, although the ADH activity was maintained after the heat treatment. This is inconsistent with the hypothesis that preservation of the secondary structure maintains ADH activity. Therefore, we focused on the direct interaction between PGDs and ADH, analyzed by differential scanning calorimetry (DSC) measurements.

(insert **Fig. 5**)

To evaluate the intermolecular interaction at 60°C, DSC measurements were performed. **Table 2** summarizes the calculated calorimetric enthalpy (ΔH_{cal}), which represents the total heat energy uptake by ADH undergoing the unfolding transition, the calorimetric entropy (ΔS_{cal}), and the mid-point temperature of the unfolding process (T_m).

The addition of PGD-G2 and G3 decreased ΔH_{cal} in the order of PGD-G3 > G2, whereas that of PGD-G1 increased ΔH_{cal} slightly. The T_m values decreased in the presence of PGDs, particularly PGD-G2. These results suggest that PGD-G2 and G3 induced the unfolding of ADH. Because the condition of water is considered to determine the state of protein denaturation and stabilization[11], we focused on water conditions that can be estimated by nuclear magnetic relaxation studies[41, 42].

(insert Table 2)

Bound water plays an important role in protein folding, protein interactions, and protein adsorption phenomena. In general, water is a strong competitor toward binding hydrophilic groups, and different hydrophilic surfaces of substances for protein interaction contain different amounts of bound water that must be replaced, removed, or/and rearranged when energy is supplied[43]. The water condition was evaluated by measuring the osmolarity of PGD-G1, G2, G3, or glycerol in 50 mM Tris–HCl buffer (pH 8.0)) in the presence and absence of ADH. As shown in **Fig. 6 (a)**, the osmolarity of the sample in the absence of ADH increased with increasing concentration of hydroxyl groups in PGDs or glycerol in the order of glycerol > PGD-G1 > PGD-G2 > PGD-G3, indicating that osmolarity is not dependent on the concentration of hydroxyl groups but rather on the molecular weight of the PGD (M_n of PGD-G1, G2, and G3 is 356, 801, and 1,690, respectively). Similar results were observed in the presence of 0.1 mM ADH (**Fig. 6 (b)**). All the PGD solutions became turbid over 1 M hydroxyl group, and thus, there were no data above 1 M (**Fig. 6 (b)**). These results suggest that the concentration of free water molecules decreased with the generation of PGDs, even in the presence of ADH.

(insert **Fig. 6**)

The properties of free and bound water in the presence of PGD were also evaluated by T_1 measurements in a mixture of D_2O/H_2O (95:5)[44]. Figure 7 shows the T_1 values as a function of the number of PGD hydroxyl groups per water molecule (N_{OH}). An increase in the generation of PGDs decreased the T_1 values for the same N_{OH}, indicating that the higher is the generation of PGDs, the tighter the water is bound to the PGDs.

(insert Fig. 7)

A model of fast exchange between a bound and unbound water fraction is often used to explain T_1. This model is based on the following equation (1)[44]:

$$R_1 = p_f R_{1f} + p_b R_{1b} \qquad (1)$$

where R_1 is the observed mean relaxation rate defined by $R_1 = 1/T_1$, R_{1f} and R_{1b} are the intrinsic relaxation rates of the unbound and bound water compartments, and p_f and p_b are the ratio of the unbound and bound water, respectively. In combination with $p_f + p_b = 1$, eq (1) can be rewritten as the following equation (2):

$$R_1 = N_b(R_{1b} - R_{1f})N_O + R_{1f} \qquad (2)$$

where the constant N_b in eq (2) is equal to the number of bound water molecules per oxygen atom and N_O is the number of oxygen atoms per water molecule. Hence, R_1 should be a linear function of N_O with slope $[N_b (R_{1b} - R_{1f})]$ if a single bound and unbound water fraction are present. In fact, the relationship between N_O and R_1 shows a linear relationship (see supporting information; Fig. SI-2) in all samples. Consequently, the slope values for glycerol, PGD-G1, G2, and G3 were calculated to be 0.026, 0.084, 0.157, and 1.553, respectively, indicating that the slope value markedly increased 18 times from PGD-G1 to G3. This means that the number of bound water molecules is critically dependent on the generation of PGDs.

Considering the results of the CD spectra (**Fig. 5**) and the DSC measurements (**Table 2**), an increased bound water content is likely to be correlated with the conformational change in ADH. In fact, PGD-G2 decreased the T_m of ADH (**Table. 2**) and showed the highest ADH activity (**Fig. 4**). Eklund *et al.* reported that water molecules are present in the catalytic site, and the water molecules are displaced by hydroxyl oxygen of ethanol in coordination with the zinc cation[45]. Taking these results and the report into account, one possible reason why the ADH activity remained in the presence of PGD-G2 and PGD-G3 is the enhanced water replacement and ethanol binding in the catalytic site, at which PGD molecules interact directly around the α-helix.

Conclusion

PGDs induced precipitation with ADH upon heating, but ADH activity was found maintained up to 67%. The optimum amount of bound water was assessed in PGD-G2, which could mediate the intermolecular interaction with ADH while maintaining the activity. This strategy is valuable for ADH recovery that can be applied in the fields of bioprocesses, biomedical, and pharmaceuticals.

Acknowledgements

This work was partially supported by a Grant-in-Aid for Scientific Research B (JSPS KAKENHI Grant Number 22300165), a Grant-in-Aid for Scientific Research on Innovative Areas "New Polymeric Materials Based on Element-Blocks (No.2401)" (JSPS KAKENHI Grant Number JP15H00748), and an Adaptable and Seamless Technology Transfer Program (A-STEP) through target-driven R & D, Contract No. AS242Z01653P from JSPS. The authors would like to thank Enago (www.enago.jp) for the English language review.

References

1. Nel AE, Madler L, Velegol D, et al. Understanding biophysicochemical interactions at the nano-bio interface. Nature Materials. 2009;8(7):543-557.
2. Liu Z, Tabakman S, Welsher K, et al. Carbon Nanotubes in Biology and Medicine: In vitro and in vivo Detection, Imaging and Drug Delivery. Nano Res. 2009;2(2):85-120.
3. Boozer C, Ladd J, Chen SF, et al. DNA-directed protein immobilization for simultaneous detection of multiple analytes by surface plasmon resonance biosensor. Anal Chem. 2006;78(5):1515-1519.
4. Ge J, Lu D, Liu Z, et al. Recent advances in nanostructured biocatalysts. Biochemical Engineering Journal. 2009;44(1):53-59.
5. Wang YJ, Caruso F. Mesoporous silica spheres as supports for enzyme immobilization and encapsulation. Chem Mater. 2005;17(5):953-961.
6. Sheldon RA. Enzyme immobilization: The quest for optimum performance. Adv Synth Catal. 2007;349(8-9):1289-1307.
7. Linse S, Cabaleiro-Lago C, Xue WF, et al. Nucleation of protein fibrillation by nanoparticles. P Natl Acad Sci USA. 2007;104(21):8691-8696.
8. Bolivar JM, Rocha-Martin J, Mateo C, et al. Stabilization of a highly active but unstable alcohol dehydrogenase from yeast using immobilization and post-immobilization techniques. Process Biochem. 2012;47(5):679-686.
9. Jain NK, Roy I. Effect of trehalose on protein structure. Protein Sci. 2009;18(1):24-36.
10. GhattyVenkataKrishna PK, Carri GA. The effect of complex solvents on the structure and dynamics of protein solutions: The case of Lysozyme in trehalose/water mixtures. Eur Phys J E. 2013;36(2).
11. Gekko K, Timasheff SN. Mechanism of protein stabilization by glycerol: preferential hydration in glycerol-water mixtures. Biochemistry-Us. 1981;20(16):4667-4676.
12. Sousa R. Use of Glycerol, Polyols and Other Protein-Structure Stabilizing Agents in Protein Crystallization. Acta Crystallogr D. 1995;51:271-277.
13. Sahu RK, Prakash V. Mechanism of prevention of aggregation of proteins: A case study of aggregation of alpha-globulin in glycerol. Int J Food Prop. 2008;11(3):613-623.
14. Vagenende V, Yap MGS, Trout BL. Mechanisms of Protein Stabilization and Prevention of Protein Aggregation by Glycerol. Biochemistry-Us. 2009;48(46):11084-11096.
15. Vera L, Czarny B, Georgiadis D, et al. Practical Use of Glycerol in Protein Crystallization. Crystal Growth & Design. 2011;11(7):2755-2762.
16. Spickermann D, Kara S, Barackov I, et al. Alcohol dehydrogenase stabilization by additives under industrially relevant reaction conditions. J Mol Catal B-Enzym. 2014;103:24-28.
17. Iyer PV, Ananthanarayan L. Enzyme stability and stabilization - Aqueous and non-aqueous environment. Process Biochem. 2008;43(10):1019-1032.
18. Obon JM, Manjon A, Iborra JL. Comparative thermostability of glucose dehydrogenase from Haloferax mediterranei. Effects of salts and polyols. Enzyme Microb Tech. 1996;19(5):352-360.
19. Calderon M, Quadir MA, Sharma SK, et al. Dendritic Polyglycerols for Biomedical Applications. Adv Mater. 2010;22(2):190-218.

20. Kurniasih IN, Keilitz J, Haag R. Dendritic nanocarriers based on hyperbranched polymers. Chem Soc Rev. 2015;44(12):4145-4164.
21. Thota BNS, Urner LH, Haag R. Supramolecular Architectures of Dendritic Amphiphiles in Water. Chem Rev. 2016;116(4):2079-2102.
22. Han YX, Qian Y, Zhou XX, et al. Facile synthesis of zwitterionic polyglycerol dendrimers with a beta-cyclodextrin core as MRI contrast agent carriers. Polym Chem-Uk. 2016;7(41):6354-6362.
23. Sousa-Herves A, Wurfel P, Wegner N, et al. Dendritic polyglycerol sulfate as a novel platform for paclitaxel delivery: pitfalls of ester linkage. Nanoscale. 2015;7(9):3923-3932.
24. Becherer T, Grunewald C, Engelschalt V, et al. Polyglycerol based coatings to reduce non-specific protein adsorption in sample vials and on SPR sensors. Anal Chim Acta. 2015;867:47-55.
25. Wu CZ, Strehmel C, Achazi K, et al. Enzymatically Cross-Linked Hyperbranched Polyglycerol Hydrogels as Scaffolds for Living Cells. Biomacromolecules. 2014;15(11):3881-3890.
26. Tschiche A, Staedtler AM, Malhotra S, et al. Polyglycerol-based amphiphilic dendrons as potential siRNA carriers for in vivo applications. J Mater Chem B. 2014;2(15):2153-2167.
27. Hellmund M, Zhou HX, Samsonova O, et al. Functionalized Polyglycerol Amine Nanogels as Nanocarriers for DNA. Macromol Biosci. 2014;14(9):1215-1221.
28. Haag R, Sunder A, Stumbé J-F. An Approach to Glycerol Dendrimers and Pseudo-Dendritic Polyglycerols. Journal of the American Chemical Society. 2000;122(12):2954-2955.
29. Lee H, Ooya T. Dendritic nanospace constructed by only glycerol units enhanced uptake of a fluorescent molecule in aqueous solution. Chemical Communications. 2012;48(4):546-548.
30. Lee H, Ooya T. Generation-Dependent Host-Guest Interactions: Solution States of Polyglycerol Dendrimers of Generations 3 and 4 Modulate the Localization of a Guest Molecule. Chem-Eur J. 2012;18(34):10624-10629.
31. Lee H, Ooya T. F-19-NMR, H-1-NMR, and Fluorescence Studies of Interaction between 5-Fluorouracil and Polyglycerol Dendrimers. Journal of Physical Chemistry B. 2012;116(40):12263-12267.
32. Ooya T, Lee H. Amino Acid-Dependent Host-Guest Interaction: Polyglycerol Dendrimer of Generation 3 Encapsulates Amino Acids Bearing Two Amino Groups. Chemnanomat. 2015;1(4):264-269.
33. Garcia-Bernabe A, Kramer M, Olah B, et al. Syntheses and phase-transfer properties of dendritic nanocarriers that contain perfluorinated shell structures. Chem-Eur J. 2004;10(11):2822-2830.
34. Yi T, Haag R, Brenn R, et al. PMMA gradient materials and in situ nanocoating via self-assembly of semifluorinated hyperbranched amphiphiles. Macromol Chem Physic. 2005;206(1):135-141.
35. Ooya T, Lee J, Park K. Effects of ethylene glycol-based graft, star-shaped, and dendritic polymers on solubilization and controlled release of paclitaxel. J Control Release. 2003;93(2):121-127.
36. Ooya T, Lee J, Park K. Hydrotropic dendrimers of generations 4 and 5: Synthesis, characterization, and hydrotropic solubilization of paclitaxel. Bioconjugate Chem. 2004;15(6):1221-1229.

37. Nouguier RM, Mchich M. Alkylation of Pentaerythritol and Trimethylolpropane, 2 Very Hydrophilic Polyols, by Phase-Transfer Catalysis. J Org Chem. 1985;50(18):3296-3298.
38. Wakuri S, Izumi J, Sasaki K, et al. Cytotoxicity Study of 32 Meic Chemicals by Colony Formation and Atp Assays. Toxicol in Vitro. 1993;7(4):517-521.
39. Pucciarelli S, Bonacucina G, Bernabucci F, et al. A Study on the Stability and Enzymatic Activity of Yeast Alcohol Dehydrogenase in Presence of the Self-Assembling Block Copolymer Poloxamer 407. Applied Biochemistry and Biotechnology. 2012;167(2):298-313.
40. Schneider G, Eklund H, Cedergrenzeppezauer E, et al. Crystal-Structures of the Active-Site in Specifically Metal-Depleted and Cobalt-Substituted Horse Liver Alcohol-Dehydrogenase Derivatives. P Natl Acad Sci-Biol. 1983;80(17):5289-5293.
41. Sterling C, Masuzawa M. Gel/Water Relationships in Hydrophilic Polymers - Nuclear Magnetic Resonance. Makromol Chem. 1968;116(Aug):140-&.
42. Quinn FX, Kampff E, Smyth G, et al. Water in Hydrogels .1. A Study of Water in Poly(N-Vinyl-2-Pyrrolidone Methyl-Methacrylate) Copolymer. Macromolecules. 1988;21(11):3191-3198.
43. Hanein D, Geiger B, Addadi L. Fibronectin Adsorption to Surfaces of Hydrated Crystals - an Analysis of the Importance of Bound Water in Protein Substrate Interactions. Langmuir. 1993;9(4):1058-1065.
44. Lusse S, Arnold K. The interaction of poly(ethylene glycol) with water studied by H-1 and H-2 NMR relaxation time measurements. Macromolecules. 1996;29(12):4251-4257.
45. Eklund H, Plapp BV, Samama JP, et al. Binding of Substrate in a Ternary Complex of Horse Liver Alcohol-Dehydrogenase. J Biol Chem. 1982;257(23):4349-4358.

Table 1. Concentrations of Samples used for T_1 Measurements in D_2O/H_2O (95:5) and N_{OH} Values Measured

N_{OH}	Glycerol (M)	PGD-G1 (M)	PGD-G2 (M)	PGD-G3 (M)
0	0	0	0	0
0.3	0.22	0.11	0.06	0.03
0.6	0.54	0.25	0.12	0.06
1.3	1.09	0.50	0.25	0.12
3.5	2.50	1.04	0.50	0.24

Table 2. Thermodynamic Parameters of ADH Determined by DSC Measurements

Samples[a]	ΔH_{cal} (kJ/mol)	ΔS_{cal} (kJ/mol·K)	T_m (°C)
ADH	307.0	0.9	54.8
ADH + PGD-G1	346.3	1.1	52.3
ADH + PGD-G2	188.5	0.6	42.3
ADH + PGD-G3	178.5	0.8	51.1

[a] Final concentration of ADH was 0.7 μM, which was dissolved in 10 mM PBS (pH 7.4). PGD-G1, G2 and G3 were added to the ADH solution (final concentration: 1 wt %).

Figure Captions

Figure 1 Chemical structures of polyglycerol dendrimer (PGD) of (a) generation 1 (PGD-G1), (b) generation 2 (PGD-G2), and (c) generation 3 (PGD-G3).

Figure 2 Cytotoxicity of PGD-G2 and G3. The cytotoxicity was evaluated by colony formation assay using V79 cells. The number of colonies per well was measured with a multipurpose high-speed image analyser.

Figure 3 Turbidity change due to ADH (10 μM) in 50 mM Tris-HCl buffer (pH 8.0) at 60 °C in the presence of (a) PGD-G1, (b) G2, (c) G3, (d) glycerol (5 wt%), and (e) in the absence of any additive.

Figure 4 Residual activity of ADH, calculated by comparing ADH activity before and after heat treatment, in the suspension (black bar) and the supernatant (diagonal-dashed bar) of samples heated at 60 ℃ for 2 h in the presence of glycerol (ADH + Gly), PGD-G1 (ADH + G1), PGD-G2 (ADH + G2) or PGD-G3 (ADH + G3) (Mean ± S.D., n = 4). ADH activity was measured by absorbance at 340 nm in 50 mM Tris-HCl buffer (pH 8.0) containing 1 μM ADH, 100 μM NAD^+, 20 μM $ZnCl_2$, and 0.5 wt% of each polymer. Asterisks indicate significant differences between ADH and ADH with each PGD sample, determined by the student *t*-test ($P<0.05$).

Figure 5 Δ[θ] calculated from CD spectra of ADH (0.7 μM) in 50 mM Tris-HCl buffer (pH 8.0) at 60 °C in the presence of 5 wt% PGD-G1 (square), G2 (triangle), G3 (circle), and without PGDs (diamond).

Figure 6 Osmolarity of PGD-G1 (square), G2 (triangle), G3 (circle) and glycerol (diamond) dissolved in 50 mM Tris-HCl buffer (pH 8.0) (a) in the absence and (b) the presence of ADH (0.1 mM).

Figure 7 The T_1 values of PGD-G1 (square), G2 (triangle), G3 (circle) and glycerol (diamond) dissolved in a mixture of D_2O/H_2O (95:5).

1

2 Fig. 1

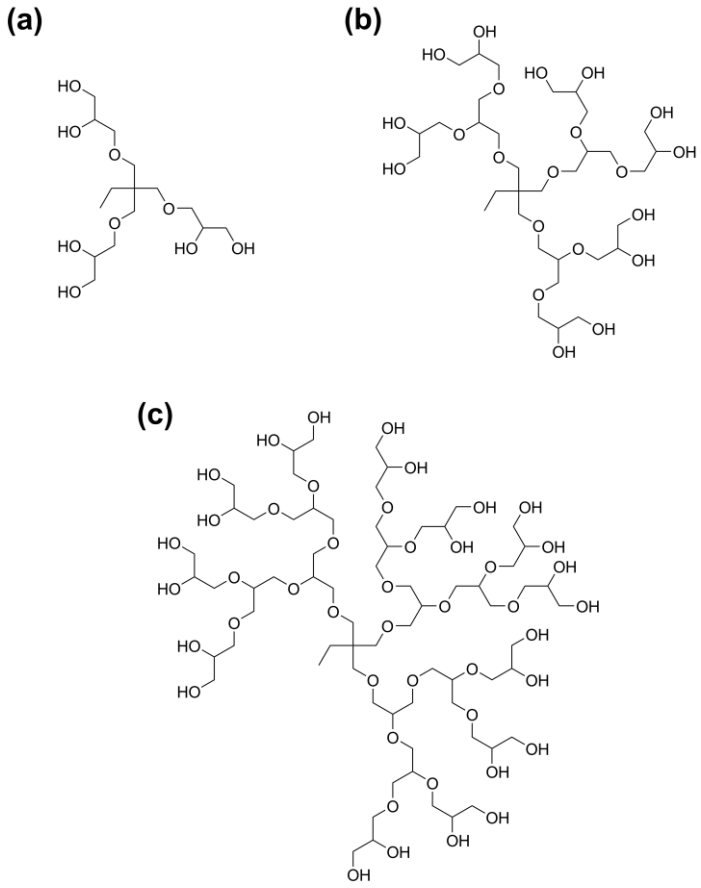

3

4

1 Fig. 2

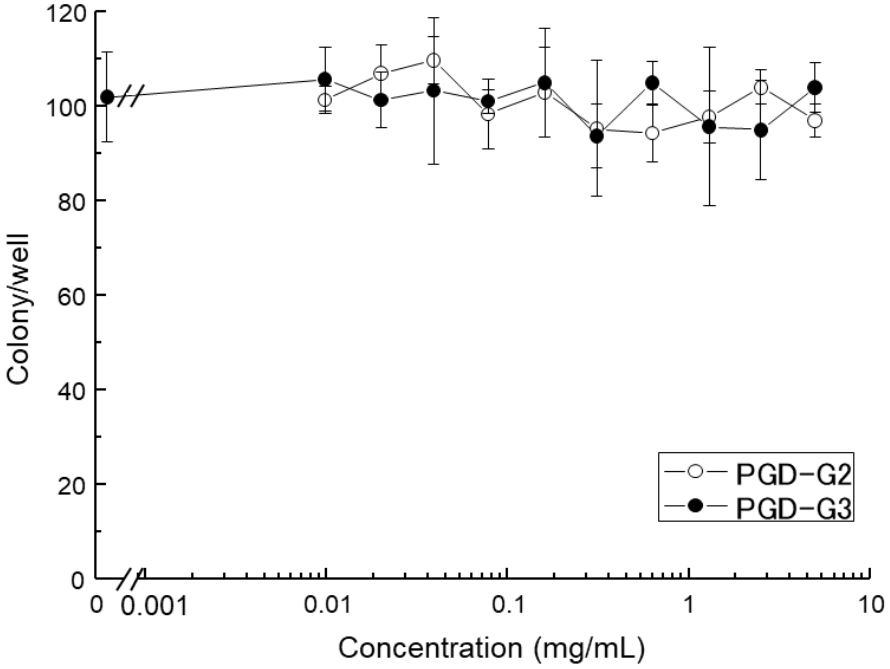
120
100
80
60
40
20
0
Colony/well
0
0.001
0.01
0.1
1
10
Concentration (mg/mL)
PGD-G2
PGD-G3

2

1 Fig. 3

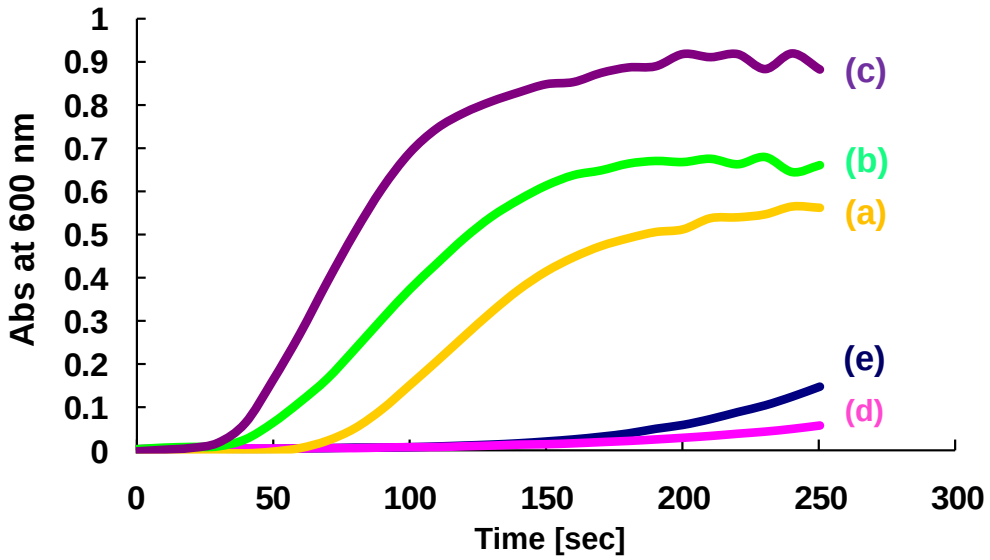
Abs at 600 nm
1
0.9
0.8
0.7
0.6
0.5
0.4
0.3
0.2
0.1
0
0
50
100
150
200
250
300
Time [sec]
(c)
(b)
(a)
(e)
(d)

2

3

1 Fig.4

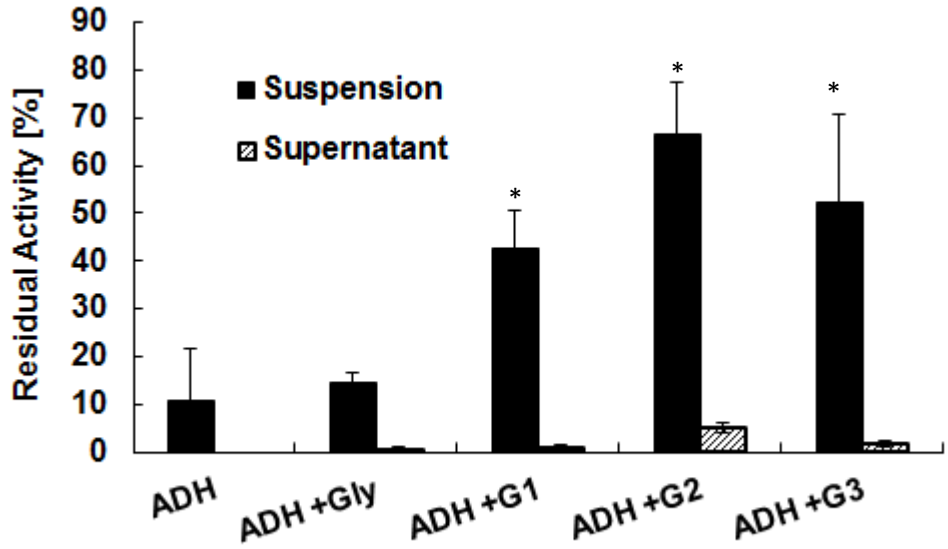
Residual Activity [%]
90
80
70
60
50
40
30
20
10
0
Suspension
Supernatant
*
*
*
ADH
ADH +Gly
ADH +G1
ADH +G2
ADH +G3

2

3

1 Fig. 5

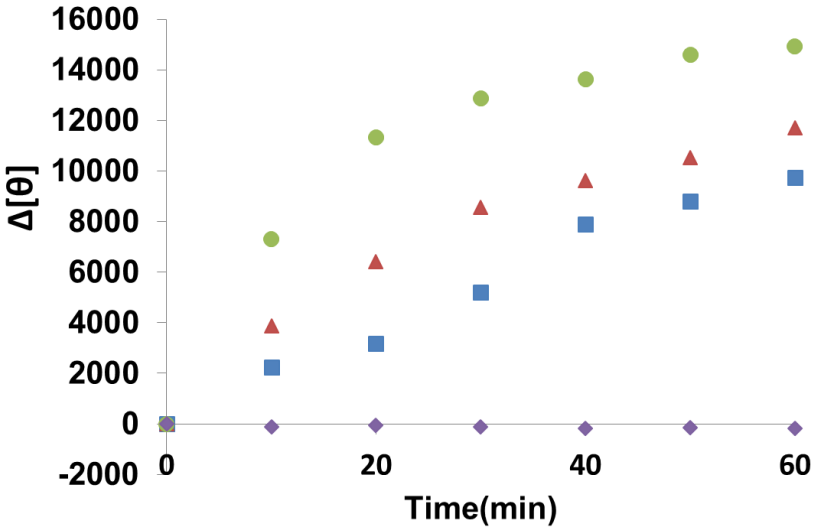
16000
14000
12000
10000
8000
6000
4000
2000
0
-2000
Δ[θ]
0
20
40
60
Time(min)

2

3

Fig. 6

(a)

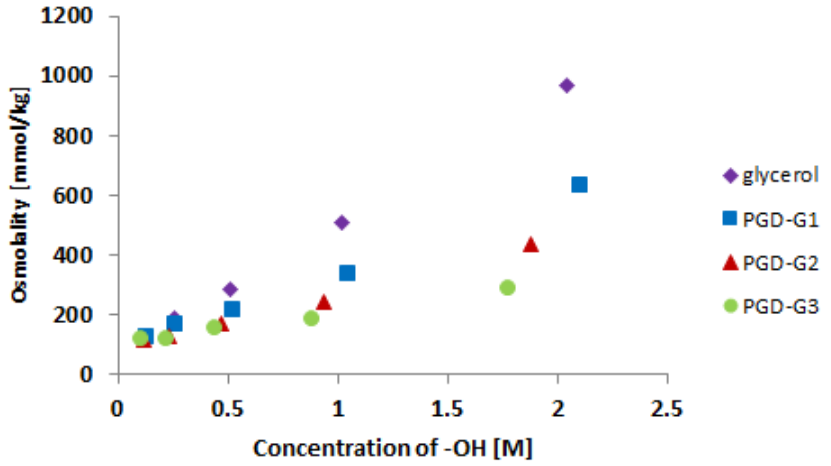
Osmolality [mmol/kg]
1200
1000
800
600
400
200
0
0
0.5
1
1.5
2
2.5
Concentration of -OH [M]
glycerol
PGD-G1
PGD-G2
PGD-G3

(b)

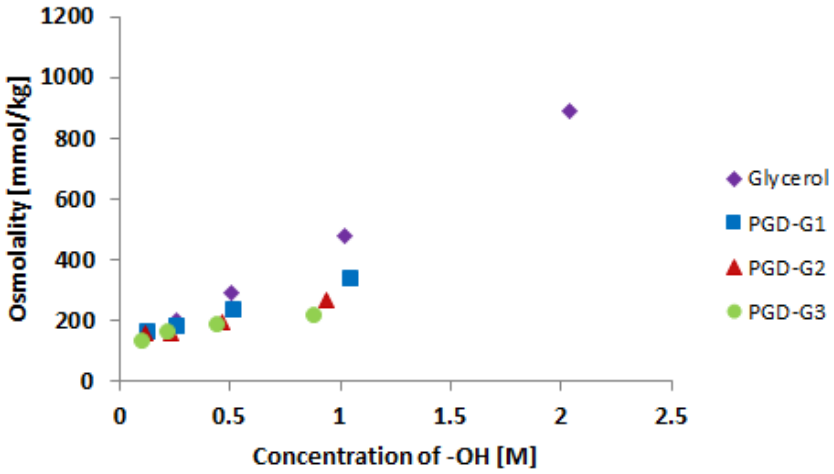
Osmolality [mmol/kg]
1200
1000
800
600
400
200
0
0
0.5
1
1.5
2
2.5
Concentration of -OH [M]
Glycerol
PGD-G1
PGD-G2
PGD-G3

1 Fig. 7

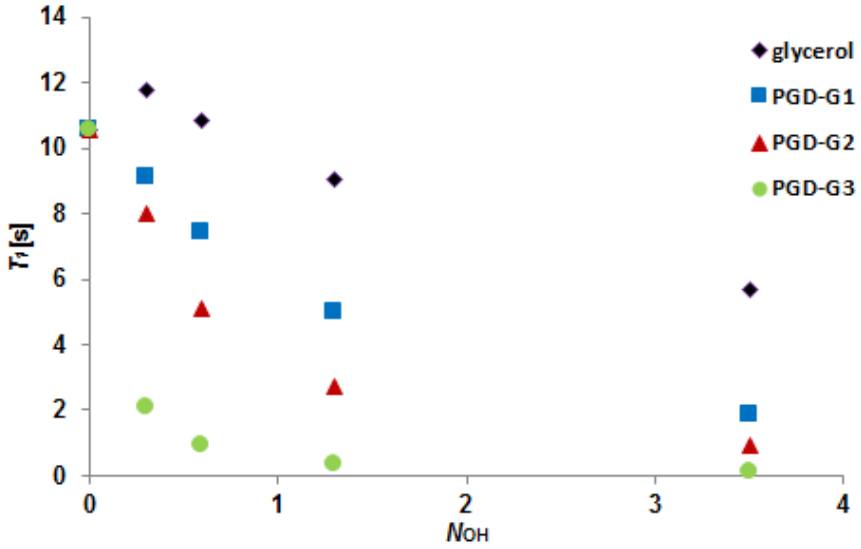

2

3

4

5

6